Monte Carlo Optimization of Depth-of-Interaction Resolution in PET Crystals

T. A. DeVol, W. W. Moses, and S. E. Derenzo

Abstract—**The light distribution along one edge of a PET scintillation crystal was investigated with a Monte Carlo simulation. This position dependent light distribution can be used to measure the 511 keV photon interaction position in the crystal on an event by event basis, thus reducing radial elongation. The predicted full width at half maximum (FWHM) of the light distribution on the 3 × 30 mm surface of a 3 × 10 × 30 mm BGO crystal surrounded by diffuse reflector is 3.0 mm. This light distribution is constant for widths (originally 3 mm) between 1 and 6 mm, but decreases from 3.0 to 1.8 mm FWHM as the height is reduced from 10 to 3 mm. Other geometrical modifications were simulated, including corner reflectors on the opposing 3 × 30 mm surface. A promising geometry is a 2.2 × 5 × 30 mm BGO crystal, for which a 2.2 mm FWHM light distribution is predicted, which should yield a PET detector module with depth of interaction measurement resolution of 3.6 mm FWHM.**

I. Introduction

THIS paper addresses how to alleviate radial elongation, a PET imaging artifact, by determining the depth of interaction of a 511 keV photon along the axis of a PET scintillation crystal. This artifact is due to 511 keV photons penetrating into adjacent crystals before undergoing an interaction. The reconstruction algorithm, having no interaction position information, assigns the interaction to the surface of the crystal closest to the patient, which is the most probable place for the interaction. This possible mispositioning results in images with a spatially variant point spread function (PSF), i.e., radial elongation. For example, the Donner 600 Crystal Tomograph has a circular PSF with a FWHM of 2.6 mm at the center of the ring which becomes an ellipse with 2.8 mm tangential × 4.8 mm radial FWHM at a radius of 10 cm [1].

The radial elongation distortion can be eliminated by measuring the photon depth of interaction in the scintillation crystal on an event by event basis and using this information in the reconstruction algorithm. While a number of methods have been proposed for performing this measurement (see the references in [2]), this paper investigates the module shown in Fig. 1, where the photomultiplier tube provides a timing pulse when a 511 keV photon interacts in one of the BGO crystals and a position sensitive photodiode determines the crystal of interaction and measures the depth of interaction. While a similar design measured a depth of interaction resolution of 11 mm FWHM for a 3 × 10 × 25 mm BGO crystal [3], simulations have shown that 5 mm FWHM depth of interaction resolution is needed to eliminate radial elongation [4].

The purpose of this paper is to use a Monte Carlo simulation to optimize the design of the detector module and achieve the requisite 5 mm FWHM depth of interaction resolution. Specific attention is paid to the distribution of scintillation light along the edge of the crystal coupled to the position sensitive detector (i.e., photodiode), as this distribution is the main factor that determines the depth of interaction resolution. This extends previous work by others that optimize either the total amount of light seen on one surface of the scintillation crystal [5], [6] or the time distribution of the detected scintillation photons [7].

II. Method

A. Monte Carlo Simulation

The detector modeled is shown in Fig. 1, with the exception that only one of the scintillation crystal/photodiode assemblies is simulated. The photomultiplier tube (PMT) is assumed to have 30% quantum efficiency and 40% reflectivity [8], while the position sensitive photodiode (PD) is assumed to have 60% quantum efficiency and 10% reflectivity. The BGO crystal was modeled with a mean free path to scatter and absorption of 400 mm [9] and an index of refraction of 2.15. The crystal was assumed to have polished surfaces that were separated by a small air gap from a diffuse reflector with 98% reflectivity. Transparent optical coupling compound having a index of refraction of 1.5 was used to couple the photodetectors to the crystal. The coordinate system used is shown in Fig. 1, with $Y = 0$ defined to be the end of the crystal that is not attached to the PMT.

The above data was used as input to DETECT [10], a Monte Carlo program developed to study light collection properties in scintillators. DETECT generates individual

Manuscript received November 8, 1991; revised December 7, 1992. This work was supported in part by the U.S. Department of Energy under contract No. DE-AC03-76SF00098, in part by Public Health Service Grants No. PO1 25840 and R01 CA48002, and in part by a grant from the Whitaker Foundation.

T. A. DeVol is with the Department of Nuclear Engineering, The University of Michigan, Ann Arbor, MI 48109-2100.

W. M. Moses and S. E. Derenzo are with the Lawrence Berkeley Laboratory, University of California, Berkeley, CA 94720.

This paper was originally presented at the 1991 IEEE Nuclear Science Symposium (NSS '91), held in Santa Fe, NM, November 5–8, 1991.

IEEE Log Number 9207249.

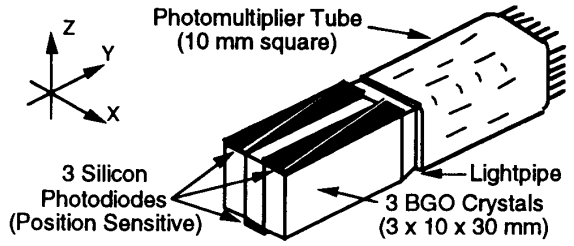

Fig. 1. Detector assembly.

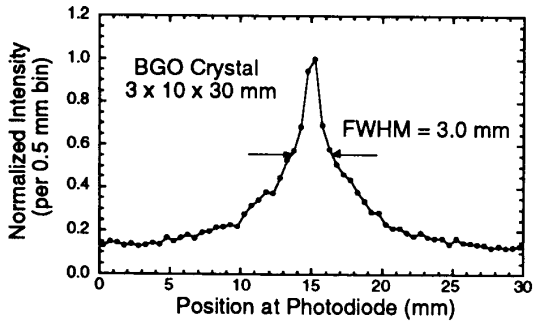

Fig. 2. Typical light distribution.

photons in a specified region in the scintillating crystal, tracks each photon in its passage through the various components and interactions with surfaces, models absorption and scatter, and records the fate (absorption, escape, or detection) of each photon. The program outputs the fraction of emitted photons that are detected by both the PMT and the PD, as well as the Y coordinate of the photons detected by the position sensitive PD.

Separate simulations are performed for all of the scintillator crystal geometries described herein. For each geometry, the first stage of the simulation is to predict the light distribution detected by the PD as a function of the position of the initial scintillation flash in the BGO crystal. Since we wish to look at emanations from a fixed depth (i.e., Y coordinate), scintillation light was "emitted" uniformly from an X–Z plane centered at this Y position. The distribution of scintillation photons detected by the PD is acquired for scintillation events at Y positions spaced every 3 mm. Fig. 2 shows the light distribution acquired in 0.5 mm bins from a $3 \times 10 \times 30$ mm BGO crystal excited at $Y = 15$ mm. The shape of the light distribution was found to be nearly independent of the excitation position (except when within a few mm from either end of the crystal), while the peak position tracked the excitation position.

The second stage of each simulation is to use these "point" (really plane) response functions, such as the one shown in Fig. 2, to estimate the depth of interaction measurement resolution of the detector module. This stage of simulation adds measurement effects to simulate the analog pulse height presented to the readout electronics when an individual 511 keV photon interacts at a fixed depth (Y position). The effects simulated are Compton interactions in the BGO crystal, the BGO light output (including statistical fluctuations), the light collection geometry of the photodiodes, and the electronic noise in the charge sensitive preamplifiers. In all cases the position sensitive photodiode was a dual wedge design, with wedges labeled "A" and "B" [3]. The "measured" interaction position is determined by computing the ratio of the signal measured by A to the total signal A + B, that is A/(A + B), which ideally would vary smoothly from 1 when excited at $Y = 0$ to 0 when excited at $Y = 30$ mm.

B. Experimental Verification

To validate our simulation, the experimental configuration in reference [3] was simulated. This was similar to the geometry shown in Fig. 1, but limitations imposed by the photodiodes required that the BGO crystal was 25 mm (rather than 30 mm) long and the PD was 20 mm (rather than 30 mm) long. The PD covered only a portion of the scintillation crystal and was positioned between $Y = 0$ and 20 mm (with the PMT at $Y = 25$ mm). The operating temperature was -100°C, so the BGO light output was 27,000 photons per MeV of deposited energy [11]. The electronic noise in each of the photodiode wedges was 275 electrons FWHM (determined by direct measurement), and the luminescent center position was smeared by 3 mm to simulate the experimentally determined spread of the electronically collimated beam of 511 keV photons.

Fig. 3 shows the experimental and simulated values of A + B and A/(A + B) as a function of the excitation position, where the error bars represent the FWHM of the A/(A + B) distribution at each position. The experimental and simulated curves have similar shapes (except for a small disagreement at positions greater than $Y =$ 20 mm, where there is no PD coverage), but the simulation consistently underestimates the width of the A/(A + B) distribution. This is thought to be a fault of the electronic circuit that computes A/(A + B), which was found to be scale sensitive (i.e., doubling the value of both A and B changed the value of A/(A + B)). The position resolution is determined by dividing the width of the A/(A + B) distribution by the slope of the A/(A + B) versus Y curve measured between 3 and 15 mm [3], yielding an experimental position resolution of 11 mm FWHM while simulation predicts 5.8 mm FWHM. This discrepancy is entirely due to the different estimates of the A/(A + B) distribution FWHM.

III. Results and Discussion

A. Theoretical Model

While scintillation light emanates from its luminescent center isotropically, its distribution on the surface of the scintillation crystal can be far from uniform; this nonuniformity is used to determine the position of the luminescent center. The nonuniformity is determined by the geometric, optical, and surface properties of the crystal, reflector, and photodetectors. The focus of this paper is to investigate the properties that change the light distribu-

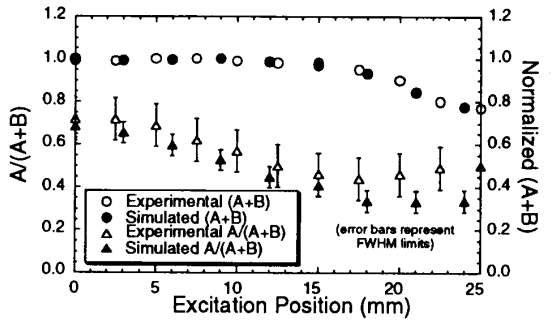

Fig. 3. Comparison of experiment and simulation.

tion along the surface of a scintillation crystal, and optimize them for measuring the axial interaction position.

When light in a medium with index of refraction n_2 is incident on a medium with lower index n_1, it undergoes total internal reflection if its angle of incidence (with respect to the surface normal) is greater than the critical angle

$$\sin(\theta_C) = n_1/n_2, \tag{1}$$

which is 27.7° for BGO ($n = 2.15$) surrounded by air. This implies that only a fraction of the scintillation photons

$$\Omega_{cone} = 0.5(1 - \cos(\theta_C)) \tag{2}$$

can directly illuminate any crystal surface [5], and these photons will only illuminate a portion of the surface, as illustrated by Fig. 4.

In a perfect rectangular parallelepiped crystal, the light exiting a given surface (and entering a photodetector placed on that surface) can be classified into three components. The first is a "direct" component, comprised of photons that are inside the light cone and directed towards the detection surface. This "direct" light forms a narrow beam that lies within a circle defined by the critical angle that is centered above the luminescent center. Direct light can be detected by a position sensitive photodetector and used to determine the position of interaction. The rest of the light, $4\pi - \Omega_{cone}$, may eventually be detected by the photodetector, but must change direction at least once before doing so. This light is termed "diffuse," and has two origins. Some photons are initially in the other 5 light cones, but exit the crystal, are scattered by the diffuse reflector, and reenter the crystal in such a way as to be detected. The remainder are photons that are initially outside the light cones, $4\pi - 6\Omega_{cone}$, and internally trapped, but scatter randomly from crystalline imperfections and are detected. The detection position of a "diffuse" photon is uncorrelated with the position of the luminescent center, and so these photons illuminate the photodiode uniformly.

This intuitive picture is corroborated by Monte Carlo simulation, and the "direct" and "diffuse" components can be seen in Fig. 2. The "direct" component forms the peak whereas the "diffuse" component forms the uniform

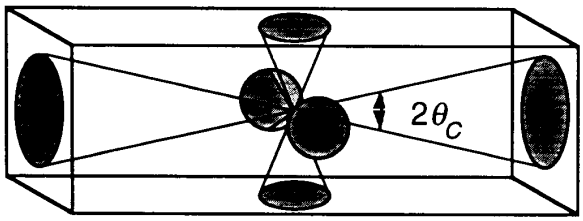

Fig. 4. Light cones as defined by the critical angle.

background under the peak. The FWHM of the "direct" light distribution is the major factor that determines the depth of interaction resolution.

B. Dependence on Crystal Size

Varying the crystal dimensions can change the diameter of the "direct" light circle on the surface, and thus affect the FWHM of the light distribution. It can also affect the total signal measured by the PMT and position sensitive PD, which must remain high so the signal to noise is sufficient for proper signal processing. The PMT signal must be large enough to generate an accurate timing signal, as well as have sufficient pulse height resolution to reject Compton scattered photons. Electronic noise is a significant fraction of the PD signal, so it is critical that the PD signal be large enough to accurately measure the interaction position. It is expected that the FWHM of the position dependent light would not vary with the crystal width (the X dimension) since the diameter of the light cone circle on the photodiode surface remains unchanged. Fig. 5 shows that this is the case, with the FWHM of the light distribution fluctuating around 3.0 mm. Fig. 5 also shows that the PMT and PD photon detection efficiencies are a constant 13% and 22% respectively.

Of greater interest is the dependence of these signals on the height (Z dimension) of the crystal. It is expected that as the height is decreased, the diameter of the light cone circle at the photodiode surface would also decrease, reducing the FWHM of the light distribution. Fig. 6 shows that as the height is decreased from 10 to 3 mm, the light distribution decreases from 3.0 to 1.8 mm FWHM. The PMT and PD photon detection efficiencies are again a roughly constant 13% and 22% respectively. Therefore, the depth of interaction measurement resolution can be improved, without degrading the PMT performance, by reducing the height (Z dimension).

C. Dependence on Surface Treatment

In some situations, the crystal size is fixed by other constraints but improved position resolution is desired, so DETECT was used to investigate the effect of surface treatments on the light distribution. The first attempt was to decrease the "diffuse" light signal (while not affecting the "direct" component) by coupling a black reflector (0% reflectivity) to the crystal surface opposite the PD. This reduced the FWHM of the light distribution from 3.0 to 2.1 mm for a $3 \times 10 \times 30$ mm BGO crystal, but also reduced the PMT and PD photon detection efficiencies to

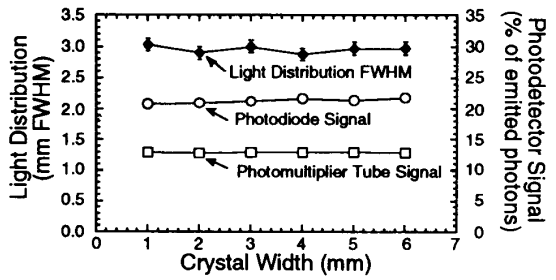

Fig. 5. Light distribution FWHM and signal amplitude versus crystal width for an $X \times 10 \times 30$ mm BGO crystal.

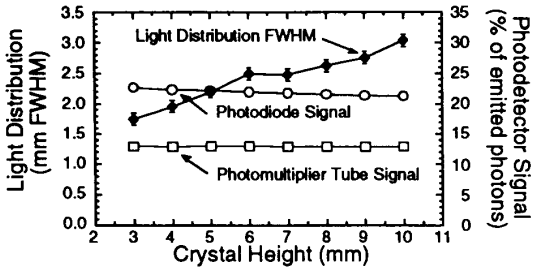

Fig. 6. Light distribution FWHM and signal amplitude versus crystal height for a $3 \times Z \times 30$ mm BGO crystal.

2.5% and 7%, respectively. Because of the electronic noise level in the PD, this loss in signal was shown experimentally to worsen the interaction position measurement resolution.

The example shows that the way to improve position resolution is to increase the "direct" light signal by converting some of the "diffuse" light into "direct" light. This was attempted by modeling a crystal whose surface opposite the PD was cut to form corner reflectors (Fig. 7), causing photons in the light cone oriented away from the PD to undergo two total internal reflections and return oriented antiparallel to their initial direction [12] which almost doubles the "direct" component of the PD signal and decreases the FWHM of the light distribution from 3.0 to 2.4 mm in a $3 \times 10 \times 30$ mm BGO crystal. The photon detection efficiency of the PD is increased to 25%, but the PMT efficiency is reduced to 7%, which is enough to provide a good timing signal and adequate energy resolution.

D. Depth-of-Interaction Measurement Resolution

Having determined the "point" spread functions for a large number of geometries, we now perform the second portion of the simulation (the determination of the depth of interaction measurement resolution as described in Section IIA) for three promising geometries—a $3 \times 10 \times 30$ mm BGO crystal, a $2.2 \times 5 \times 30$ mm crystal, and a $3 \times 10 \times 30$ mm crystal with corner reflectors as shown in Fig. 7. In all cases the crystal was coupled to 30 mm long dual wedge position sensitive PD and the A/(A + B) ratio, the FWHM of the A/(A + B) ratio, and

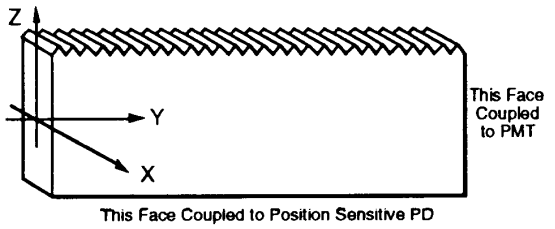

Fig. 7. Crystal with multiple corner reflectors.

the total PD and PMT signals are determined as a function of luminescent center position. Fig. 8 shows the A/(A + B) ratios for all geometries and the FWHM of the A/(A + B) ratio for one geometry—the FWHM data from the other geometries are extremely similar and are omitted to enhance legibility. In all three cases the total PD and PMT signals are effectively independent of position (< 10% variation) and large enough to ensure proper signal processing.

The position resolution is obtained by dividing the FWHM of the A/(A + B) ratio by the slope of the curve in Fig. 8. With the $3 \times 10 \times 30$ mm a 7.2 mm FWHM depth of interaction resolution is obtained, which is worse then the 5.8 mm predicted in Section IIB. This is because position information is now obtained for the entire length of the crystal rather than for only the first 20 mm, and so the slope is reduced. The resolution with this size crystal can be improved to 5.1 mm FWHM by putting corner reflectors on the edge opposite the photodiode, as a result of increased "direct" light on the photodiode. However, the best depth of interaction resolution (3.6 mm FWHM) is obtained by limiting the spread of the "direct" light by reducing the crystal size to $2.2 \times 5 \times 30$ mm. Such crystals could be combined to form an ultra-high resolution detector module similar to Fig. 1, except that each 1 cm square PMT is coupled to two rows of four BGO crystal/photodiode assemblies.

Previous predictions of the effect on depth of interaction measurement resolution on the reconstructed point spread function in a tomograph indicate that for a geometry similar to that of the Donner 600 Crystal Tomograph [1], a resolution of 5 mm FWHM is necessary to effectively eliminate radial elongation [4]. Applying a 3×30 mm PD to the edge of the $3 \times 10 \times 30$ mm BGO crystal will not meet this requirement, but placing corner reflectors on the side opposite the PD will and reducing the crystal size to $2.2 \times 5 \times 30$ mm will exceed this requirement. Although a greater fraction of incident 511 keV photons will penetrate into adjacent crystals in this last geometry, accurately measuring the interaction position should prevent the point spread function from deteriorating. However, verification requires a full Monte Carlo simulation of such a tomograph, which is beyond the scope of this paper.

IV. Conclusion

Simulations were performed of the light distribution along the edge of a PET scintillation crystal to optimize

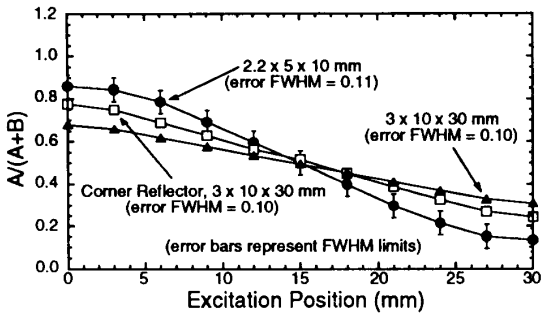

Fig. 8. $A/(A + B)$ signal as a function of axial position.

its ability to measure the 511 keV photon interaction axial position in that crystal. A $3 \times 10 \times 30$ mm BGO crystal surrounded by a diffuse reflector is predicted to yield a depth of interaction position resolution of 7.2 mm FWHM. This resolution is reduced to 3.6 mm at a crystal height of 5 mm, but is not affected by changing the width. The total amount of light detected on any surface is essentially unchanged by any of these modifications. Cutting numerous corner reflectors into the 3×30 mm surface of a $3 \times 10 \times 30$ mm crystal will improve the position resolution to 5.1 mm FWHM, but will reduce the light on the 3×10 mm surface by 50%. The multiple corner reflector and $2.2 \times 5 \times 30$ mm geometries both show promise as elements for an ultra-high resolution PET detector module designed to eliminate the radial elongation artifact.

ACKNOWLEDGMENTS

T. A. DeVol thanks the Environmental Restoration and Waste Management Fellowship Program, which is administered by Oak Ridge Associated Universities for the U.S. Department of Energy, for support, and W. W. Moses thanks The Whitaker Foundation for support.

REFERENCES

[1] S. E. Derenzo, R. H. Huesman, J. L. Cahoon, *et al.*, "A positron tomograph with 600 BGO crystals and 2.6 mm resolution," *IEEE Trans. Nucl. Sci.*, vol. NS-35, pp. 659–664, 1988.

[2] P. Bartzakos and C. J. Thompson, "A depth-encoded PET detector," *IEEE Trans. Nucl. Sci.*, vol. NS-38, pp. 732–738, 1991.

[3] S. E. Derenzo, W. W. Moses, H. G. Jackson, *et al.*, "Initial characterization of a position-sensitive photodiode/BGO detector for PET," *IEEE Trans. Nucl. Sci.*, vol. NS-36, no. 1, pp. 1084–1090, 1989.

[4] W. W. Moses, R. H. Huesman, and S. E. Derenzo, "A new algorithm for using depth-of-interaction measurement information in PET data acquisition," *J. Nucl. Med.*, vol. 32, no. 5, p. 995, 1991.

[5] W. A. Shurcliff and R. C. Jones, "The trapping of fluorescent light produced within objects of high geometrical symmetry," *J. Opt. Soc. Am.*, vol. 39, no. 11, pp. 912–916, 1949.

[6] C. Carrier and R. LeComte, "Effects of geometrical modifications and crystal defects on the light collection in ideal rectangular parallelepipedic BGO scintillators," *Nucl. Instr. Meth.*, vol. A294, pp. 355–364, 1990.

[7] S. I. Ziegler and H. Ostertag, *et al.*, "Effects of scintillation light collection on the time resolution of a time-of-flight detector for annihilation quanta," *IEEE Trans. Nucl. Sci.*, vol. NS-37, pp. 574–579, 1990.

[8] W. D. Gunter, Jr., G. R. Grant, and S. A. Shaw, "Optical devices to increase photocathode quantum efficiency," *Appl. Opt.*, vol. 9, no. 2, pp. 251–257, 1970.

[9] S. E. Derenzo and J. K. Riles, "Monte Carlo calculation of the optical coupling between Bismuth germanate crystals and photomultiplier tubes," *IEEE Trans. Nucl. Sci.*, vol. NS-29, no. 1, pp. 191–195, 1982.

[10] G. F. Knoll, T. F. Knoll, and T. M. Henderson, "Light collection in scintillation detector composites for neutron detection," *IEEE Trans. Nucl. Sci.*, vol. 35, no. 1, pp. 872–875, 1988.

[11] M. J. Weber and R. R. Monchamp, "Luminescence of $Bi_4Ge_3O_{12}$: Spectral and decay properties," *J. Appl. Phys.*, vol. 4, pp. 5495–5499, 1973.

[12] J. Karp and G. Muehllehner, "Performance of a position-sensitive scintillation detector," *Phys. Med. Bio.*, vol. 30, pp. 643–655, 1985.